

# The Stereoselectivities in Aminoacidatoethylenediamineoxalatocobalt (III) Complexes

メタデータ	言語: eng 出版者: 公開日: 2017-10-03 キーワード (Ja): キーワード (En): 作成者: 藤波, 修平, 柴田, 村治 メールアドレス: 所属:
URL	<a href="https://doi.org/10.24517/00011237">https://doi.org/10.24517/00011237</a>

This work is licensed under a Creative Commons  
Attribution-NonCommercial-ShareAlike 3.0  
International License.



## The Stereoselectivities in Aminoacidatoethylenediamine-oxalatocobalt(III) Complexes

Yoichi OGATA, Shuhei FUJINAMI, and Muraji SHIBATA

*Department of Chemistry, Faculty of Science, Kanazawa University*

(Received December 10, 1980)

**Abstract** The  $[\text{Co}(\text{ox})(\text{L-am})(\text{en})]$ - type complexes have been prepared and separated into four stereoisomers by means of chromatographic procedure. They have been characterized by their absorption, CD and PMR spectra. Their observed CD spectra have been analyzed to the configurational and vicinal CD curves, which have indicated to hold the additivity rule for the present system. The stereoselectivities have been classified into two groups; one is that between diastereoisomers and another is that between geometrical isomers with the same absolute configuration. The former have been found for several pairs of the diastereoisomers, while the latter have been found for the most of pairs of the geometrical isomers. These results have suggested the significance of the interactions between a side-chain of a chelated aminoacidate ligand and another chelated ligand.

### Introduction

Metal complexes containing optically active amino acids frequently exhibit stereoselective effects on the formations of their diastereoisomers. In order to investigate such stereoselectivity, the mixed ligand cobalt(III) complexes containing L- or D-aspartic acid as the primary ligand were previously chosen in our laboratory<sup>1-5)</sup>, and the observed stereoselectivities were explained in terms of the interaction between the  $\beta$ -carboxylate group of aspartate ion and another ligand coordinated.

In the present work,  $[\text{Co}(\text{ox})(\text{L-am})(\text{en})]$ - type complexes consisting of oxalate (ox), L-aminoacidate (L-am), and ethylenediamine (en) were prepared in order to investigate extensively stereoselective effects of L-am, using L-alanine (L-Ala), L-valine (L-Val), L-isoleucine (L-iLeu), L-threonine (L-Thr), L-methionine (L-Met), and L-serine (L-Ser).

### Experimental

*Preparation.* The procedures for the  $[\text{Co}(\text{ox})(\text{L-Hasp})(\text{en})]$  complex<sup>1)</sup> were modified

the procedures for the  $[\text{Co}(\text{ox})(\text{L-ala})(\text{en})]$  complex. The reaction conditions were taken as temperature  $40^\circ\text{C}$ ,  $\text{pH} \sim 9.5$  and reaction time 36 h. The separation was carried out by use of a column containing 200~400 mesh Dowex 50W-X8 resin  $\text{Na}^+$  form ( $5.0 \times 60.0\text{cm}$ ). By elution with water, three desired bands appeared (labeled A-1, A-2 and A-3 in turn). The A-1, after concentration to a small volume, was poured onto a column containing Shephadex G-15 ( $2.6 \times 100.0\text{cm}$ ). After several hours' elution with water, a considerably broadened band produced was collected in a number of fractions (every 3ml). With the front fractions, the main CD peak showed (+) sign, while (-) sign was found with the rear ones. The portions of the fractions exhibiting distinctive (+) or (-) sign were collected, and they were rechromatographed up to the main CD peaks showed constant intensities. From those fractions of the A-1 (+), A-1(-), A-2 and A-3, four isomeric complexes were crystallized.

The preparation and separation of the isomers of the  $[\text{Co}(\text{ox})(\text{L-val})(\text{en})]$  complex were carried out similarly to the above, and two bands descended were labeled B-1 and B-2 in turn. The B-1 and B-2 fractions were then rechromatographed with a Sephadex G-15 column and a Dowex 50W-X8 column, respectively, whereby diastereoisomeric pairs, B-1(+) and B-1(-), and B-2(+) and B-2(-), were obtained.

The  $[\text{Co}(\text{ox})(\text{L-ileu})(\text{en})]$ ,  $[\text{Co}(\text{ox})(\text{L-thr})(\text{en})]$ ,  $[\text{Co}(\text{ox})(\text{L-met})(\text{en})]$  and  $[\text{Co}(\text{ox})(\text{L-ser})(\text{en})]$  complexes were all prepared and separated by the same procedure as that of the L-ala complex, and every four bands could be obtained in the chromatographic separations, labeled C-1~C-4, D-1~D-4, E-1~E-4 and F-1~F-4 for the L-ileu, L-thr, L-met and L-ser complexes, respectively.

*Reaction Conditions.* The conditions such as reaction time, temperature, pH and solvent were varied in the experiment with the L-ser complex. The formation ratios among the stereoisomers were evaluated from the spectral data of the isolated complexes.

*Measurements.* The absorption spectra were measured with a Hitachi 323 Recording Spectrophotometer. The CD spectra were recorded on a JASCO J-40CS automatic recording spectropolarimeter with JASCO Model J-DPZ data processor. The measurements of PMR spectra were carried out with a JEOL Model JNM-PS-100 or a FX-100 spectrometer (100MHz) at about  $25^\circ\text{C}$ , using  $\text{D}_2\text{O}-\text{D}_2\text{SO}_4$  (ca. 30%) solvent. Sodium  $\text{D}_4$ -trimethylsilylpropionate (TMSP) was taken as the internal standard.

## Results and Discussion

*Characterization.* The results of elemental analyses, and the absorption and CD spectral data for the isolated complexes are summarized in Table 1. For a  $[\text{Co}(\text{ox})(\text{L-am})(\text{en})]$ -type complex, there are four stereoisomers. The geometrical forms (*mer* and *fac*) were determined from the absorption spectra, and the absolute configurations ( $\Lambda$  and  $\Delta$ ) by the signs of the main CD peaks in the first absorption band region. The

TABLE 1. ELEMENTAL ANALYSES, ABSORPTION AND CD SPECTRAL DATA

Label	Complex	Elemental anal., % <sup>a1</sup>			Band I		Band II		CD	
		C	H	N	$10^{-3} \bar{\nu}_{max} \text{ cm}^{-1} \epsilon_{max}$	$10^{-3} \bar{\nu}_{max} \text{ cm}^{-1} \epsilon_{max}$	$10^{-3} \bar{\nu}_{max} \text{ cm}^{-1} \Delta \epsilon_{max}$	$10^{-3} \bar{\nu}_{max} \text{ cm}^{-1} \Delta \epsilon_{max}$	$10^{-3} \bar{\nu}_{max} \text{ cm}^{-1} \Delta \epsilon_{max}$	
A-1(+)	<i>mer</i> - $\Lambda$ - [Co(ox)(L-ala)(en)] • 2H <sub>2</sub> O	25.27 (25.39)	5.45 (5.48)	12.77 (12.69)	19.3	95	27.0	175	17.8 20.7	+ 1.72 + 1.07
A-1(-)	<i>mer</i> - $\Delta$ - [Co(ox)(L-ala)(en)] • 2H <sub>2</sub> O	25.19 (25.39)	5.28 (5.48)	12.44 (12.69)	19.3	95	27.0	175	17.7 21.0	- 2.03 - 1.30
A-2	<i>fac</i> - $\Delta$ - [Co(ox)(L-ala)(en)] • 1.5H <sub>2</sub> O	26.29 (26.10)	5.19 (5.32)	13.07 (13.04)	19.3	149	27.2	163	18.8	- 3.89
A-3	<i>fac</i> - $\Lambda$ - [Co(ox)(L-ala)(en)] • 2.8H <sub>2</sub> O	24.38 (24.32)	5.69 (5.72)	12.13 (12.16)	19.3	149	27.2	163	18.7	+ 3.38
B-1(+)	<i>mer</i> - $\Lambda$ - [Co(ox)(L-val)(en)] • 1.7H <sub>2</sub> O	30.75 (30.55)	6.09 (6.10)	11.47 (11.88)	19.3	104	26.9	189	18.1 19.8	+ 1.65 + 1.40
B-1(-)	<i>mer</i> - $\Delta$ - [Co(ox)(L-val)(en)] • 1.2H <sub>2</sub> O	31.37 (31.32)	5.88 (5.96)	11.94 (12.17)	19.2	91	26.9	172	17.7 20.8	- 2.60 - 1.45
B-2(-)	<i>fac</i> - $\Delta$ - [Co(ox)(L-val)(en)] • 3.5H <sub>2</sub> O	27.85 (27.99)	6.01 (6.52)	10.81 (10.88)	19.1	167	27.2	181	18.9	- 3.89
B-2(+)	<i>fac</i> - $\Lambda$ - [Co(ox)(L-val)(en)] • 1.4H <sub>2</sub> O	30.97 (31.02)	6.01 (6.02)	12.16 (12.06)	19.3	165	27.1	177	18.6	+ 3.28
C-1	<i>mer</i> - $\Lambda$ - [Co(ox)(L-ileu)(en)] • 1.2H <sub>2</sub> O	33.45 (33.47)	6.31 (6.29)	11.67 (11.71)	19.3	95	27.0	171	18.1 19.8	+ 1.52 + 1.36
C-2	<i>mer</i> - $\Delta$ - [Co(ox)(L-ileu)(en)] • 1.5H <sub>2</sub> O	32.96 (32.97)	6.00 (6.36)	11.49 (11.54)	19.2	100	29.6	187	17.7 20.8	- 2.93 - 1.66
C-3	<i>fac</i> - $\Delta$ - [Co(ox)(L-ileu)(en)] • 1.2H <sub>2</sub> O	33.57 (33.47)	6.36 (6.29)	11.46 (11.71)	19.3	151	27.2	164	18.9	- 4.18
C-4	<i>fac</i> - $\Lambda$ - [Co(ox)(L-ileu)(en)] • 0.7H <sub>2</sub> O	34.26 (34.33)	5.77 (6.17)	11.98 (12.01)	19.1	144	27.1	169	18.6	+ 2.52
D-1	<i>mer</i> - $\Delta$ - [Co(ox)(L-thr)(en)] • 0.7H <sub>2</sub> O	28.34 (28.45)	4.88 (5.19)	12.18 (12.44)	19.3	96	26.9	173	17.7 20.7	- 2.50 - 1.50
D-2	<i>mer</i> - $\Lambda$ - [Co(ox)(L-thr)(en)] • 2.0H <sub>2</sub> O	26.40 (26.60)	5.23 (5.58)	11.69 (11.63)	19.3	97	27.0	181	17.9 20.3	+ 1.50 + 0.94
D-3	<i>fac</i> - $\Lambda$ - [Co(ox)(L-thr)(en)] • 0.7H <sub>2</sub> O	28.49 (28.45)	5.15 (5.19)	12.47 (12.44)	19.2	152	27.2	170	18.7	+ 3.34
D-4	<i>fac</i> - $\Delta$ - [Co(ox)(L-thr)(en)]	29.94 (29.55)	4.64 (4.96)	12.41 (12.92)	19.3	157	27.2	171	18.9	- 4.25
E-1	<i>mer</i> - $\Lambda$ - [Co(ox)(L-met)(en)] • 1.0H <sub>2</sub> O	29.15 (28.95)	5.33 (5.41)	11.05 (11.26)	19.2	95	26.9	181	17.9 20.4	+ 1.85 + 1.20
E-2	<i>mer</i> - $\Delta$ - [Co(ox)(L-met)(en)] • 1.0H <sub>2</sub> O	29.08 (28.95)	5.39 (5.41)	11.18 (11.26)	19.3	93	26.8	174	17.7 20.8	- 2.15 - 1.35
E-3	<i>fac</i> - $\Delta$ - [Co(ox)(L-met)(en)] • 2.6H <sub>2</sub> O	27.04 (26.88)	5.45 (5.82)	9.89 (10.45)	19.2	147	27.2	174	18.8	- 3.50
E-4	<i>fac</i> - $\Lambda$ - [Co(ox)(L-met)(en)] • 1.0H <sub>2</sub> O	29.02 (28.95)	5.25 (5.41)	11.08 (11.26)	19.2	147	27.2	171	18.7	+ 3.70
F-1	<i>mer</i> - $\Delta$ - [Co(ox)(L-ser)(en)] • 2.1H <sub>2</sub> O	24.08 (24.09)	4.98 (5.26)	11.72 (12.04)	19.2	96	27.0	177	17.7 20.7	- 2.35 - 1.40
F-2	<i>mer</i> - $\Lambda$ - [Co(ox)(L-ser)(en)] • 1.5H <sub>2</sub> O	24.86 (24.86)	5.11 (5.07)	12.40 (12.43)	19.2	98	27.0	173	17.8 20.6	+ 1.54 + 0.97
F-3	<i>fac</i> - $\Lambda$ - [Co(ox)(L-ser)(en)] • 1.0H <sub>2</sub> O	25.55 (25.54)	4.90 (4.90)	12.83 (12.77)	19.2	148	27.2	163	22.9	+ 3.57
F-4	<i>fac</i> - $\Delta$ - [Co(ox)(L-ser)(en)] • 0.1H <sub>2</sub> O	26.86 (26.87)	4.33 (4.57)	13.35 (13.43)	19.2	155	27.2	168	23.1	- 3.75

a) ( ): calcd.

absorption and CD spectra for the L-ileu complex are illustrated in Fig. 1. The absorption and CD spectra for the other complexes showed similar features to those of the L-ileu complex.

It is known that the observed CD spectrum of a complex with an optically active ligand can be separated into two curves due to the configurational and vicinal contributions<sup>6,7</sup>. The separated curves with the present complexes are shown in Figs. 2 and 3, respectively, from which it is seen that the configurational CD curves are substantially similar to one another, irrespective of the chelated L-am, indicating that the additivity rule holds for the present system. The vicinal CD curves due to the chelated L-ams consist chiefly of negative components in the first absorption band region. The vicinal CD curves for the L-ileu and L-thr complexes suggest that the second asymmetry on chelated ligand is almost regardless of CD spectra.

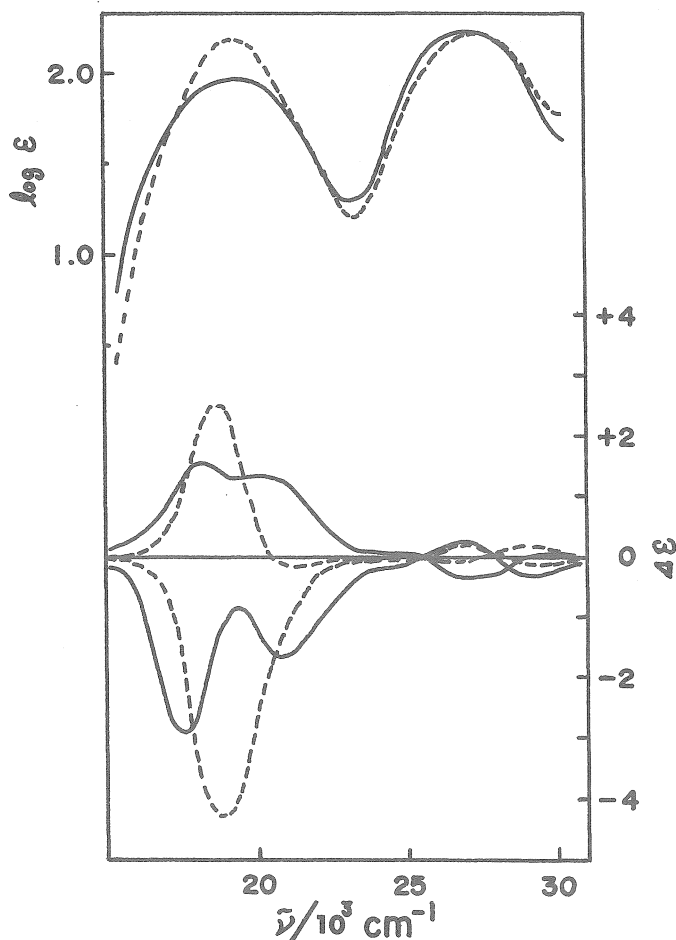


Fig. 1. Absorption and CD spectra of ;  
 — *mer*-[Co(ox)(L-ileu)(en)] and  
 - - - *fac*-[Co(ox)(L-ileu)(en)] .

*Stereoselectivity.* The formation ratios represented by percentages among the stereoisomers of the present complexes are given in Table 2, in which the previously reported results for related complexes<sup>1,2)</sup> are also included for comparison.

In the present system, since activated charcoal was used, the equilibrations among the stereoisomers are considered to be accomplished<sup>8,9)</sup>. The formation ratios observed are considered from the following two points of view; the stereoselectivity between the diastereoisomers ( $\Lambda$  and  $\Delta$ ) and that between the geometrical isomers (*mer* and *fac*) with the same absolute configuration ( $\Lambda$  or  $\Delta$ ).

We assume three factors governing the formation ratios among the stereoisomers in the present system; (a) electrostatic repulsion among the donor atoms, (b) interaction between the polar side-chain of chelated L-am and the  $-\text{NH}_2$  or  $-\text{COO}^-$  group of another chelated ligand, and (c) steric hindrance due to the bulky substituent of a

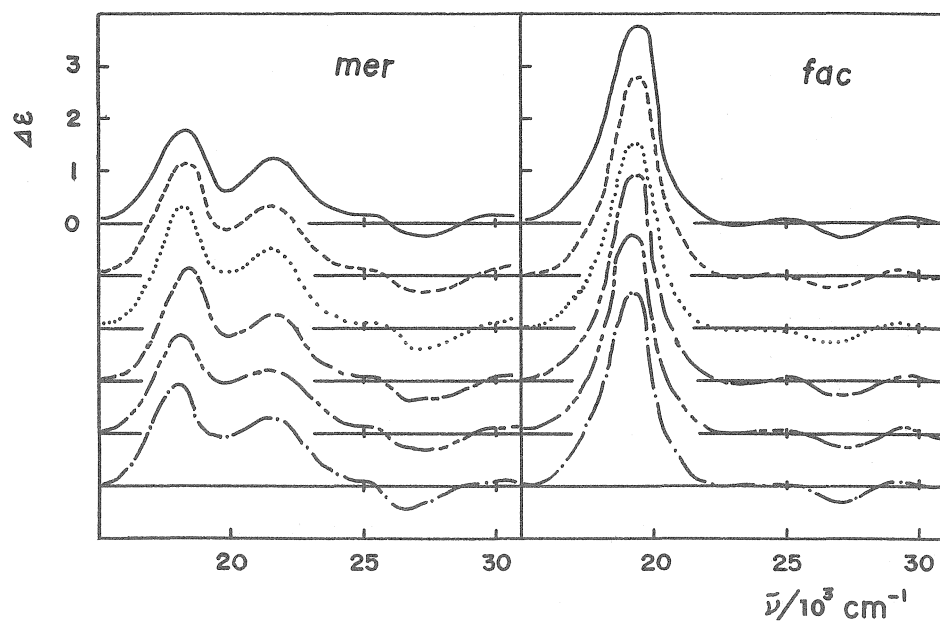


Fig. 2. Configurational CD curves of ;  
 —L-ala, - - - -L-val, ······L-ileu,  
 - · - · -L-thr, - - - -L-met and · - · -L-ser complexes.

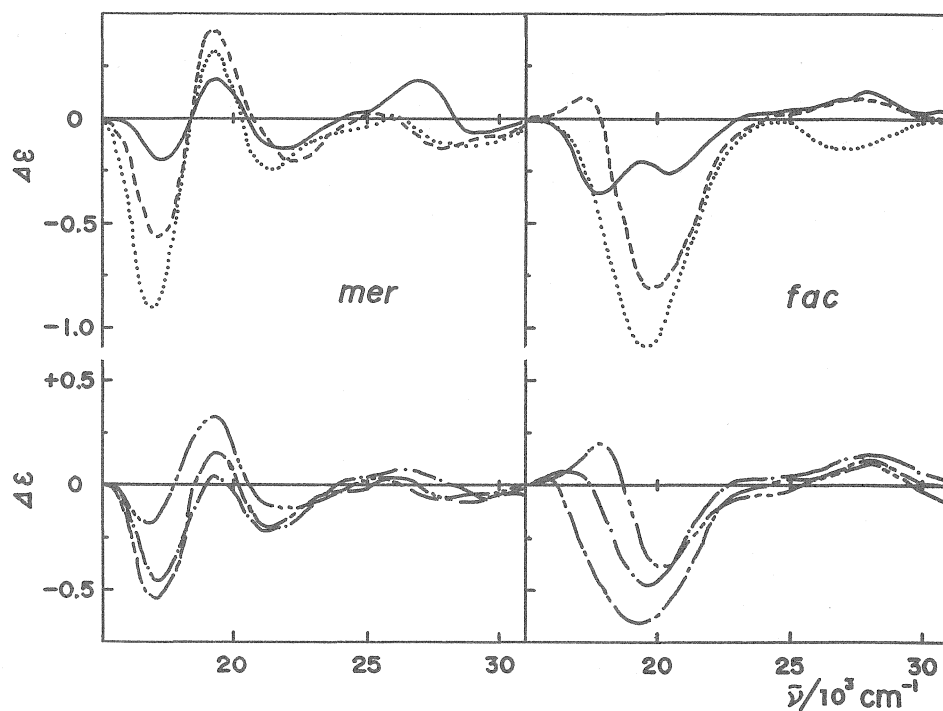


Fig. 3. Vicinal CD curves of ;  
 —L-ala, - - - -L-val, ······L-ileu,  
 - · - · -L-thr, - - - -L-met and · - · -L-ser complexes.

TABLE 2. FORMATION RATIOS AMONG STEREOISOMERS

Complex	<i>mer</i> - $\Lambda^a$	<i>mer</i> - $\Delta^a$	<i>fac</i> - $\Lambda^a$	<i>fac</i> - $\Delta^a$
[Co(ox)(L-ala)(en)]	37 (1)	44 (2)	8 (4)	11 (3)
[Co(ox)(L-val)(en)]	44 (1)	37 (2)	5 (4)	14 (3)
[Co(ox)(L-ileu)(en)]	48 (1)	34 (2)	5 (4)	13 (3)
[Co(ox)(L-thr)(en)]	25 (2)	59 (1)	10 (3)	6 (4)
[Co(ox)(L-met)(en)]	35 (1)	44 (2)	11 (4)	10 (3)
[Co(ox)(L-ser)(en)]	26 (2)	54 (1)	13 (3)	8 (4)
[Co(ox)(L-Hasp)(en)] <sup>b)</sup>	11 (2)	72 (1)	14 (3)	3 (4)
[Co(ox)(L-Hglu)(en)] <sup>b)</sup>	32	48	11	9
[Co(ox)(L-leu)(en)] <sup>b)</sup>	35	49	8	8
[Co(ox)(L-aspNH <sub>2</sub> )(en)] <sup>c)</sup>	62 (1)	19 (2)	14 (3)	5 (4)

a) ( ): elution order on chromatography. b) Ref. 1.

c) Ref. 2.

chelated L-am. These assumptions seem to be reasonable on the basis of various experimental facts.<sup>1,2,10,11)</sup>

The stereoselectivities between the diastereoisomers are given in Table 3 for the  $\Delta$  forms. It is found that the *fac*-L-val, *fac*-L-ileu, *mer*-L-thr and *mer*-L-ser complexes exhibit about 70%. In the complexes containing the L-am which has no polar side-chain, the stereoselectivities can be explained by the factor (c); the steric hindrance of a bulky substituent against the -NH<sub>2</sub> group of ethylenediamine is larger than that against the -COO<sup>-</sup> group of oxalate, and this is supported by the PMR spectra of the *fac*-L-leu complex as is seen in Fig. 4. The  $\Lambda$  isomer having the substituent near to the -NH<sub>2</sub> group shows two doublets for -CH<sub>3</sub> signal, while the  $\Delta$  isomer having the substituent near to the -COO<sup>-</sup> group shows only one doublet. This differences can be understood by considering that the steric hindrance prevents free rotation of isopropyl

TABLE 3. STEREOSELECTIVITIES

Complex	<i>mer</i> - $\Delta^a$	<i>fac</i> - $\Delta^a$	<i>mer</i> - $\Lambda^b$	<i>mer</i> - $\Delta^b$
[Co(ox)(L-ala)(en)]	54	59	82	80
[Co(ox)(L-val)(en)]	46	73	90	73
[Co(ox)(L-ileu)(en)]	41	71	91	73
[Co(ox)(L-thr)(en)]	71	39	71	91
[Co(ox)(L-met)(en)]	56	47	76	82
[Co(ox)(L-ser)(en)]	68	37	67	87
[Co(ox)(L-Hasp)(en)] <sup>c)</sup>	87	18	44	96
[Co(ox)(L-Hglu)(en)] <sup>c)</sup>	60	45	74	84
[Co(ox)(L-leu)(en)] <sup>c)</sup>	58	50	81	86
[Co(ox)(L-aspNH <sub>2</sub> )(en)] <sup>d)</sup>	77	26	58	93

a) Stereoselectivity between diastereoisomers.

b) Stereoselectivity between geometrical isomers with the same absolute configuration.

c) Ref. 1.

d) Ref. 2.

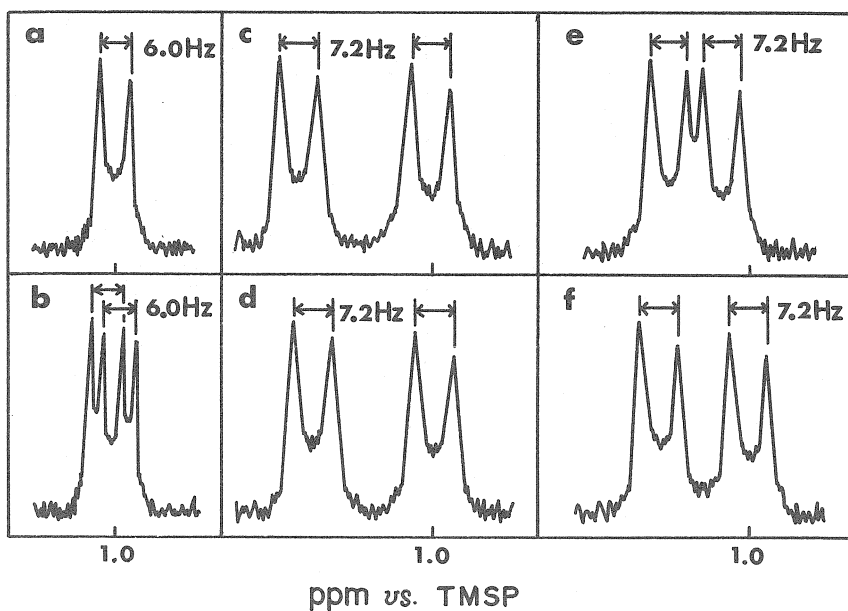


Fig. 4. PMR spectra of ;

- a) *fac*- $\Delta$ -L-leu, b) *fac*- $\Lambda$ -L-leu, c) *mer*- $\Delta$ -L-val,  
 d) *mer*- $\Lambda$ -L-val, e) *fac*- $\Delta$ -L-val and f) *fac*- $\Lambda$ -L-val isomeric complexes.

TABLE 4. SEPARATION DISTANCE BETWEEN CH<sub>3</sub> SIGNALS

Complex	<i>mer</i> - $\Lambda$	<i>mer</i> - $\Delta$	<i>fac</i> - $\Lambda$	<i>fac</i> - $\Delta$
[Co(ox)(L-val)(en)]	25Hz	23Hz	10Hz	17Hz
[Co(ox)(L-leu)(en)]	—	3Hz	2Hz	0Hz

group for the  $\Lambda$  isomer. Thus, it is expected to form *fac*- $\Delta$  and *mer*- $\Lambda$  isomers stereoselectively for the complexes having nonpolar side-chain of L-am. The PMR spectra of the L-val complex (Fig. 4) suggest that the steric hindrance in the [Co(ox)(L-am)(en)] system is the largest for the structure having branched  $\beta$ -carbon on the chelated L-am side-chain (we call this as  $\beta$ -branched structure), since the four stereoisomers show all two doublets for -CH<sub>3</sub> signal. And then, it may be considered that the L-val complex has more rigid structure with respect to the chelated L-val compared with other complexes. Thus, the L-val complex seems to exhibit larger stereoselectivity than the L-leu one. The situation may be the same for the L-ileu complex, because L-ileu has  $\beta$ -branched structure. On the PMR spectra, the separation distances between the two -CH<sub>3</sub> signals for the L-val and L-leu complexes are given in Table 4. It is found from Tables 2 and 4 that the larger distance exhibits the larger formation ratio for each of the complexes. In the L-val and L-ileu complexes, the stereoselectivities of the *mer* isomers are smaller than those of the *fac* ones. The reason can be understood by the orientation of hydrogen atoms on the chelated ethylenediamine as is seen in Fig. 5. One

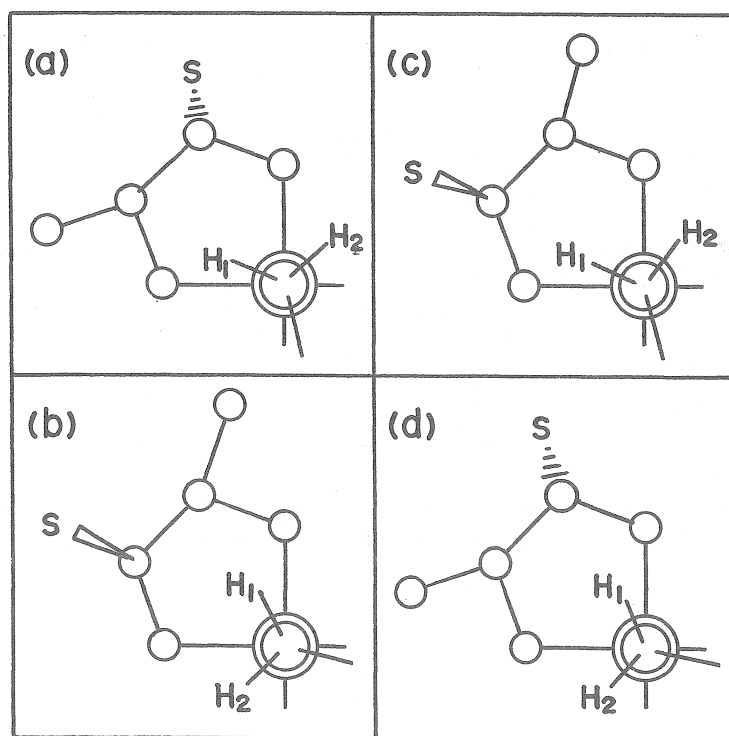


Fig. 5. Orientation of hydrogen atoms on ethylenediamine of ;  
 a) *mer*- $\Lambda$ , b) *mer*- $\Delta$ , c) *fac*- $\Lambda$  and d) *fac*- $\Delta$  stereoisomers.  
 S: Substituent.

of the hydrogen atoms on the apical  $-\text{NH}_2$  group of ethylenediamine directs to the aminoacidate substituent for *fac* isomers. Thus, the difference of steric hindrance between diastereoisomers is larger for the *fac* isomers than for the *mer* ones.

In the complexes containing L-am with polar side-chain, L-thr and L-ser complexes, the observed stereoselectivities are understood by the factor (b). In the *mer* isomers, the effects of (b) may be regarded as an attractive force through hydrogen-bonding (H-bonding) mediated by water molecule pictured in Fig. 6, because the addition of ethanol to the aqueous system resulted in the reduction of the stereoselectivity (see Table 5). It is considered that the hydrogen bonding prefers to the  $-\text{NH}_2$  group of ethylenediamine than to the  $-\text{COO}^-$  group of oxalate. This effect has been supported in the cases of the L-Hasp<sup>1)</sup> and L-aspNH<sub>2</sub><sup>2)</sup> complex. The hydrogen bonding effect will lead the stereoselective formation of the *mer*- $\Delta$  and *fac*- $\Lambda$  isomers. As to the *fac*- $\Lambda$  isomers, however, the stereoselectivities were unnoticed compared with *mer*- $\Delta$  isomers. It seems that there is no interaction between the polar side-chain and water molecule for the *fac*- $\Lambda$  isomers (Table 5).

The stereoselectivities between the geometrical isomers with the same absolute configuration (Table 3) can be understood by factors (a), (b) and (c), in analogy with the

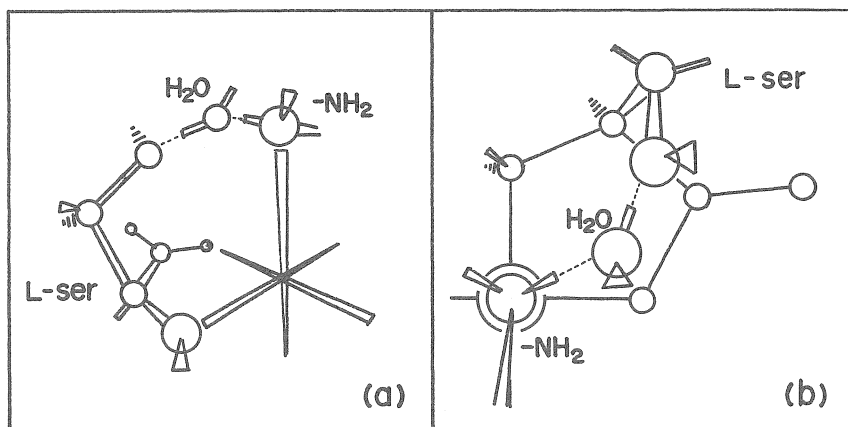


Fig. 6. Formation of hydrogen bonding mediated water molecule for  $[\text{Co}(\text{ox})(\text{L-ser})(\text{en})]$ . The hydrogen bonding is pictured from (a) horizontal side and (b) apical side.

TABLE 5. SOLVENT EFFECTS OF ETOH ON STEREOSELECTIVITY BETWEEN THE DIASTEREOISOMERS FOR  $[\text{Co}(\text{ox})(\text{L-ser})(\text{en})]$  COMPLEX

$\text{H}_2\text{O}/\text{EtOH}(\text{V}/\text{V})$	<i>mer</i> - $\Delta$	<i>fac</i> - $\Delta$
10	67	36
7.5	66	34
5	64	36
3	61	37
2	61	36

above mentioned stereoselectivities between the diastereoisomers, the factor (a) being the most significant. For example, as to the L-val complex having  $\beta$ -branched structure it can be explained as follows; the preferential formation of the *mer* isomer, compared with the *fac* one, is evidently due to (a), and the difference of the stereoselectivity between the  $\Lambda$  and  $\Delta$  isomers is due to (c), that is, a hydrogen atom on the  $-\text{NH}_2$  group of ethylenediamine directs, for the *fac*- $\Lambda$  isomer, to the L-am substituent (Fig. 5). Thus, the difference of steric hindrance between the *mer* and *fac* isomers is larger for the  $\Lambda$  configuration than that for the  $\Delta$  one. The stereoselectivities between the geometrical isomers with the same absolute configuration for the  $\Lambda$ -ser,  $\Lambda$ -asp $\text{NH}_2$  and  $\Lambda$ -Hasp complexes are less than those of the other complexes. These facts may be arisen from strong interaction, factor (b), due to hydrogen bonding.

The data on the stereoselectivities between the diastereoisomers for the L-ser complex under various conditions are given in Tables 5 and 6. These results showed that the conditions used for Preparation (40°C, pH 9.5, 36 h and in  $\text{H}_2\text{O}$ ) were in fact adequate conditions in order to investigate the stereoselectivities in the present system.

*Elution Order.* It is found from Table 2 that the observed elution order among

TABLE 6. STEREOSELECTIVITIES IN [Co(ox)(L-ser)(en)] UNDER VARIOUS CONDITIONS

		<i>mer</i> - $\Delta$	<i>fac</i> - $\Delta$
Time (h)	0.5	50	46
	4	60	43
	32	68	36
	128	68	37
Temperature (°C)	4	55	44
	15	58	38
	40	68	37
	60	66	36
pH	3.5	69	36
	7.5	69	36
	9.5	68	37

stereoisomers is approximately parallel to the order of the formation ratios. This trend can be explained in terms of dipole moment.<sup>3,12)</sup> It seems reasonable to assume that a stereoisomer having smaller dipole moment is eluted prior to a stereoisomer having larger one in the use of Dowex 50W-X8 resin. On the other hand, it seems also reasonable to assume that a stereoisomer with smaller dipole moment is formed more predominantly by the factor (a).

#### References

- 1) M. Takeuchi and M. Shibata, *Bull. Chem. Soc. Jpn.*, **47**, 2797 (1974).
- 2) H. Takenaka and M. Shibata, *Bull. Chem. Soc. Jpn.*, **49**, 2133 (1976).
- 3) K. Kawasaki, J. Yoshii, and M. Shibata, *Bull. Chem. Soc. Jpn.*, **43**, 819 (1970).
- 4) T. Matsuda, T. Okumoto, and M. Shibata, *Bull. Chem. Soc. Jpn.*, **45**, 802 (1972).
- 5) T. Matsuda and M. Shibata, *Bull. Chem. Soc. Jpn.*, **46**, 3104 (1973).
- 6) B. E. Douglas and S. Yamada, *Inorg. Chem.*, **4**, 1561 (1965).
- 7) N. Matsuoka, J. Hidaka, and Y. Shimura, *Inorg. Chem.*, **9**, 719 (1970).
- 8) F. P. Dwyer and F. L. Garvan, *J. Am. Chem. Soc.*, **83**, 2610 (1961).
- 9) G. H. Searle, F. R. Keen, and S. F. Lincoln, *Inorg. Chem.*, **17**, 2362 (1978).
- 10) K. Kawasaki and M. Shibata, *Bull. Chem. Soc. Jpn.*, **40**, 236 (1967).
- 11) R. G. Dening and N. C. Payne, *J. Chem. Soc.*, **1969**, 1197.
- 12) S. Tsuge, "Bunshi no Kozo to Bunrikino", Kagaku Zokan 69, A. Takahashi, A. Takizawa, and Y. Yamashita, Kagakudojin, Kyoto (1976), 15.